Energy Storage Materials 24 (2020) 412–416

Contents lists available at ScienceDirect

Energy Storage Materials

journal homepage: www.elsevier.com/locate/ensm

A molten battery consisting of Li metal anode, $AlCl_3$-LiCl cathode and solid electrolyte

Jialiang Lang [a,1], Kai Liu [a,1], Yang Jin [b,1], Yuanzheng Long [a], Longhao Qi [a], Hui Wu [a,*], Yi Cui [c,d,**]

[a] State Key Lab of New Ceramics and Fine Processing, School of Materials Science and Engineering, Tsinghua University, Beijing, 100084, China
[b] School of Electrical Engineering, Zhengzhou University, Zhengzhou, 450001, China
[c] Department of Materials Science and Engineering, Stanford University, Stanford, CA, 94305, USA
[d] Stanford Institute for Materials and Energy Sciences, SLAC National Accelerator Laboratory, 2575 Sand Hill Road, Menlo Park, CA, 94025, USA

ARTICLE INFO

Keywords:
High temperature battery
AlCl3-LiCl||LLZTO||Li cell
Stationary energy storage

ABSTRACT

High performance rechargeable batteries are urgently needed to address the demands of grid-scale stationary energy storage. High temperature battery systems, such as Na-S battery, Na-NiCl2 battery (ZEBRA battery) and liquid metal electrode (LME) battery, exhibit advantages like high power density and high cyclic stability, but also suffer from the high operating temperature. We recently invented new concept of molten lithium metal batteries, consisting of liquid lithium anodes, alloy (Sn, Bi, Pb) liquid cathodes and lithium ion conductor as solid electrolytes. Here we demonstrate a molten metal chloride battery that operates at a relatively low temperature of 210 °C. The battery has been designed to include molten (AlCl3-LiCl) cathode, solid electrolyte (garnet-type Li6.4La3Ta0.6Zr1.4O12 (LLZTO) ceramic tube) and molten lithium anode. The assembled AlCl3-LiCl||LLZTO||Li full cell has an average discharge voltage of 1.55 V and energy efficiency of 83% and has been successfully cycled for 100 cycles (800 h) without capacity fade. The theoretical specific energy of cell is 350 Wh/kg and the estimated cost is $11.6/kWh based on the weight of electrode materials. Considering the high performance, high safety, low operating temperature and low cost of raw materials, our new type of molten-electrode battery system opens up new opportunities for stationary energy storage.

Large-scale electrochemical energy storage system is critical for the renewable energy and smart grid technologies [1–3]. In particular, rechargeable batteries with low cost, long lifespan, good safety and high power density are required for stationary energy storage [4–6]. Many types of batteries technologies are being developed, examples including traditional lead-acid batteries [7], Li-ion batteries [8–10], Al-ion batteries [11,12], and flow batteries [13,14]. However, such room-temperature batteries suffer from high cost or limited lifespan, which seriously restricts their applications in stationary energy storage [15,16]. Recently, high-temperature batteries, including Na-S battery [17] and liquid metal electrode (LME) battery [18], have become an area of focus since they potentially meet the performance requirements for the smart electric grid. However, the exceedingly high operation temperature (>300 °C), which results in safety hazards and high maintenance cost, still remains as serious problem. The ZEBRA battery (Na-$NiCl_2$) can be operated at a relatively low temperature (250 °C), however, the high cost of Ni cathode severely limits its practical applications [19,20]. Therefore, a new molten rechargeable battery for large-scale energy storage, which can be operated at a relative low temperature with an acceptable cost, is still challenging.

Recently, our team developed a new-type LME battery using LLZTO ceramic tube as solid electrolyte, which can operate at a relative low temperature of 240 °C [21]. In the first demonstration, we show a battery chemistry system consisting of molten Bi-Sn-Pb alloying cathodes and molten Li metal anodes with theoretical specific energy limited to 230 Wh/kg. Herein, we designed a new high temperature battery chemistry with much higher theoretical specific energy and lower cost, which consists of $AlCl_3$-LiCl molten salt cathode, solid electrolyte tube (garnet-type $Li_{6.4}La_3Ta_{0.6}Zr_{1.4}O_{12}$ (LLZTO) ceramic tube) and liquid lithium anode. The $AlCl_3$-LiCl||LLZTO||Li full cell delivered a high cyclic performance and an acceptable power/energy density with a relative low cost. Besides, the relative low operating temperature and low

* Corresponding author.
** Corresponding author. Department of Materials Science and Engineering, Stanford University, Stanford, CA, 94305, USA.
E-mail addresses: huiwu@tsinghua.edu.cn (H. Wu), yicui@stanford.edu (Y. Cui).
[1] These authors contributed equally to this work.

https://doi.org/10.1016/j.ensm.2019.07.027
Received 3 April 2019; Received in revised form 11 July 2019; Accepted 18 July 2019
Available online 23 July 2019

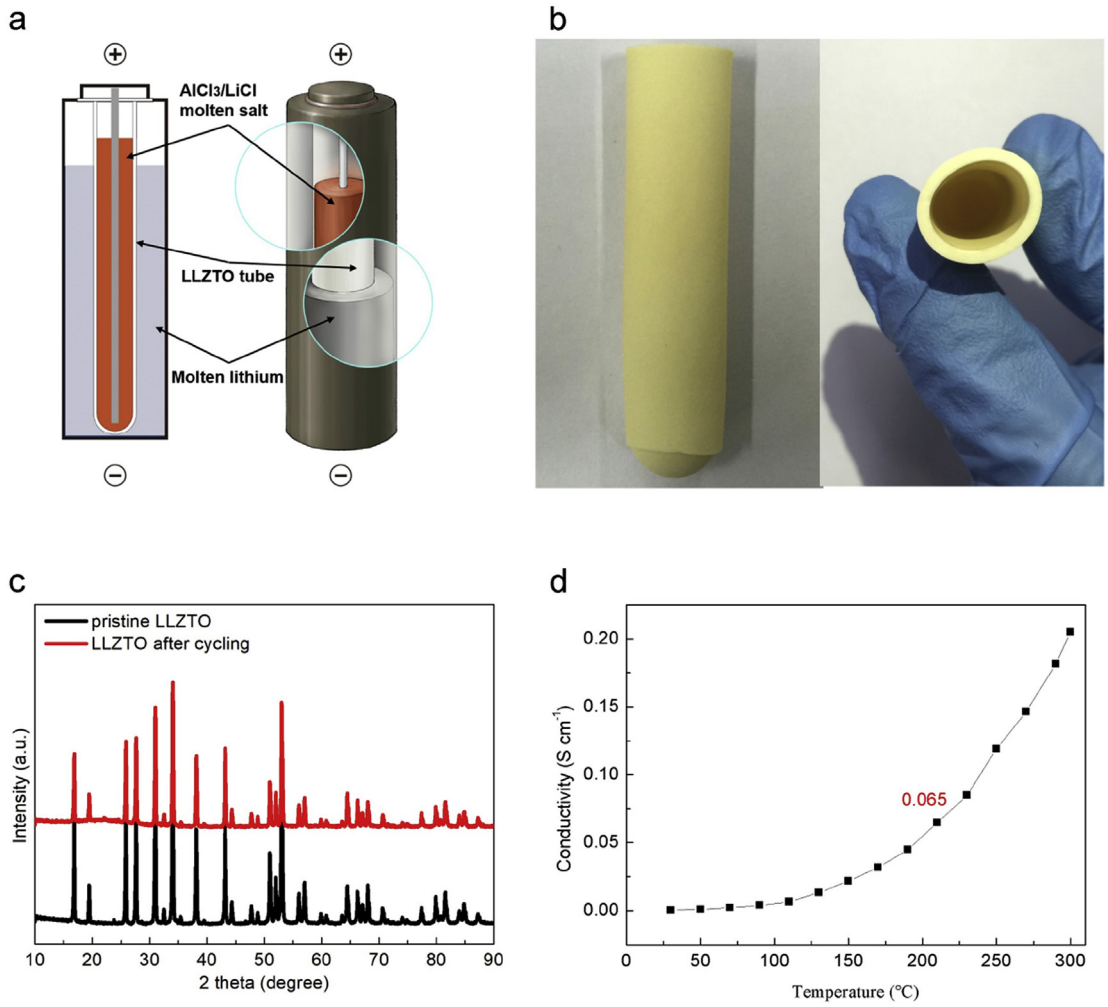

Fig. 1. (a) The construction of the Li||LLZTO||$AlCl_3$-LiCl cell. (b) Digital photos of the LLZTO ceramic tube. (c) XRD pattern of the LLZTO ceramic tube before and after cycling. (d) Ionic conductivity of LLZTO ceramic from 30 to 300 °C.

flammability of the cathode materials ensure the high safety of the full cell. Therefore, the new-designed $AlCl_3$-LiCl||LLZTO||Li full cell is a promising candidate for stationary energy storage.

We design the battery with $AlCl_3$-LiCl cathode, LLZTO solid electrolyte and lithium anode. We selected the $AlCl_3$-LiCl as cathode with the following design thinking in mind: 1) The Li-$AlCl_3$ redox couple is a promising candidate owing to its high theoretical specific capacity (520.7 mAh g^{-1}). 2) The $AlCl_3$-LiCl system have a low melting point of 110 °C. 3) The $AlCl_3$ materials have much lower cost compared with other metal chlorides, like $NiCl_2$. The price of Al is only 15% of the price of Ni. 4) The corrosion of the above molten salt system is much lower than the system containing Ni^{2+} and Fe^{3+}, which provides more economical material choices used for cathode current collectors and cell cases [22]. The overall redox reaction of the $AlCl_3$-LiCl||LLZTO||Li battery is as follow:

$$LiAlCl_4 + 3\ Li \leftrightarrow Al + 4\ LiCl\ (E_0 = 1.68\ V\ at\ 210\ oC) \quad (1)$$

The theoretical specific energy based on the active materials is 686 Wh/kg. We emphasize that our battery system exhibits high safety owing to the relatively low operating temperature and the non-flammable cathode materials. In a Na-S battery, the failure of Al_2O_3 electrolyte or internal shorting of battery will lead to severe safety hazard caused by the short-time high temperature and flammability of molten sulphur. As a comparison, the $AlCl_3$-LiCl||LLZTO||Li battery system would exhibit much improved safety. Even the ceramic separators have mechanical failure, there is still no serious safety hazard. In that case, the liquid cathode salt will get into contact with the molten Li and react to form non-flammable and non-explosive LiCl and Al, which will block further reaction.

Fig. 1a shows the configuration schematic of the battery. A stainless steel cylinder was used as negative current collector, molten Li as anode, LLZTO ceramic tube (Fig. 1b,c and Fig. S1) as electrolyte, $AlCl_3$-LiCl (60:40 mole %) as cathode and aluminum foil as positive current collector. Both anode and cathode are liquid state when the cell operates at 210 °C, which ensures the good interface contact between the molten liquid electrodes and the solid electrolyte. At such temperature, the solid electrolyte also exhibits high ionic conductivity of 65 mS cm^{-1} at 210 °C (Fig. 1d), which is greater than that of most liquid organic electrolytes (ex. ~10 mS cm^{-1}, 1 M $LiPF_6$ in carbonate-based solvent at room temperature) [23]. Besides, the LLZTO tube possesses a high relative density of 99%, which can effectively prevent any leakage or crossover of the liquid electrode materials and the self-discharge [21,24–27]. The existing of LiCl in the molten salt not only lowers the melting point of the cathode materials, but also functions as a secondary electrolyte to transfer lithium ions.

The voltage profile of the first discharge was shown in Fig. 2a. There is a short plateau at ~1.8 V, which is possibly caused by the side reactions in the interfaces. The main discharge plateau was at ~1.65 V, corresponding to the cathode specific capacity of ~200 mAh g^{-1}. After the plateau, the discharge voltage rapidly fell down to the cutoff voltage (1.2 V). There was ~50% of $AlCl_3$ contributing to the reaction. As the reaction progressed, the mole ratio of the $AlCl_3$ and LiCl continuously

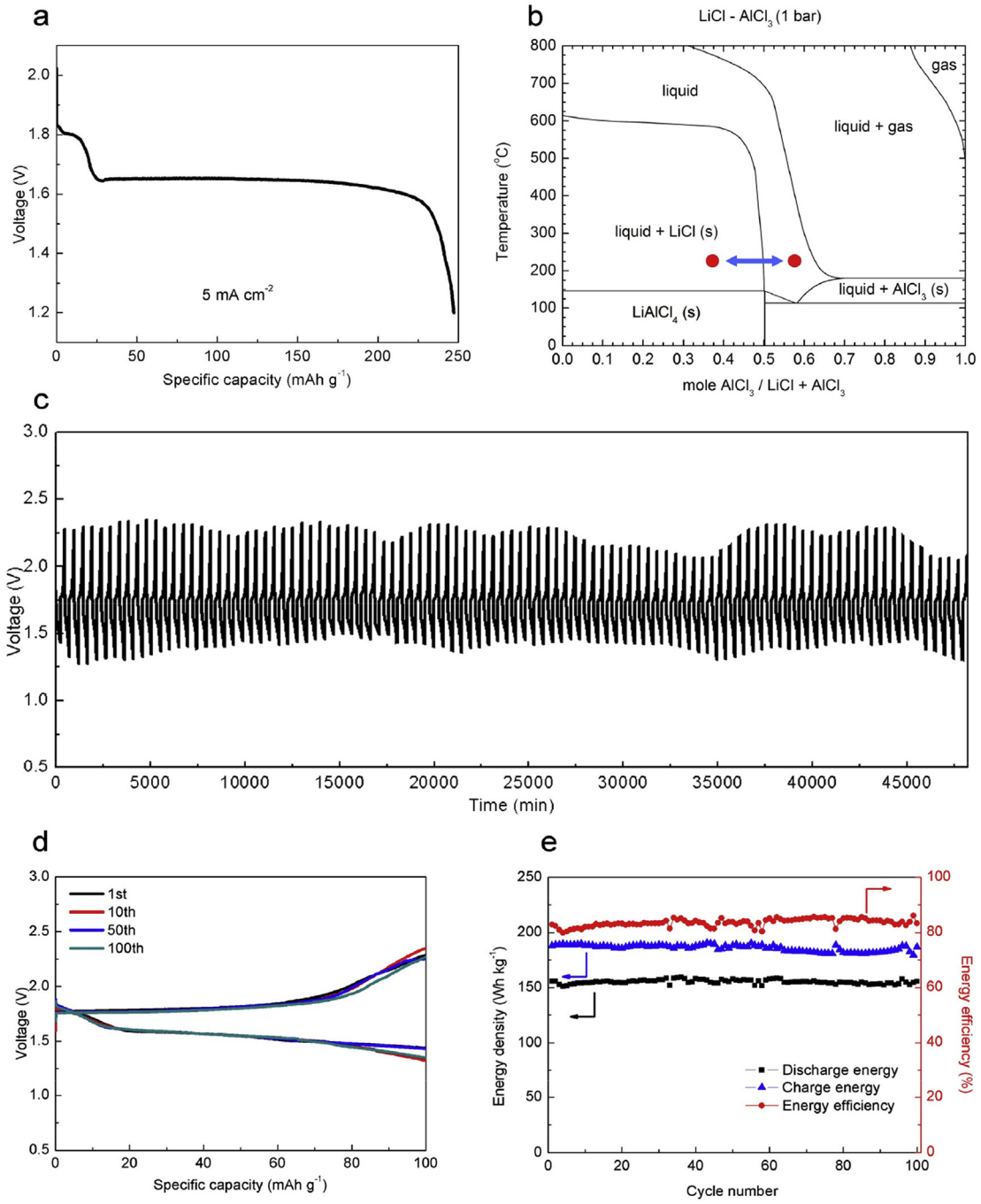

Fig. 2. (a) Voltage profile of the first discharge process at 5 mA cm^{-2}. (b) The phase change of cathode materials during cycling. (c) Voltage profiles from the 1st to the 100th discharge/charge cycle at 10 mA cm^{-2} with a specific capacity of 100 mAh g^{-1}. (d) Voltage profiles of the 1st, 10th, 50th and 100th discharge/charge cycles at 10 mA cm^{-2} with a specific capacity of 100 mAh g^{-1}. (e) Energy densities of cathode and energy efficiency as functions of cycle number from the 1st cycle to the 100th cycle at 10 mA cm^{-2} with a constant discharge/charge capacity of 100 mAh g^{-1}.

decreased, leading to the precipitation of LiCl and the reduction of the liquid phase, therefore the discharge voltage started to fall down when the specific capacity of cathode reached 230 mAh g^{-1}. Based on the weight of electrode materials, the specific energy of cell is 350 Wh/kg and the energy density per unit volume is 584.1 Wh/L. The estimated cost is $11.6/kWh.

Long lifespan is a critical factor for large-scale energy storage applications. To test the cyclic performance, an $AlCl_3$-LiCl||LLZTO||Li full cell was cycled at a current density of 10 mA cm^{-2} with a constant discharge/charge capacity of 100 mAh g^{-1} for 100 cycles (800 h). The phase change of the cathode materials during cycling was shown in Fig. 2b. During the discharge process, part of solid LiCl precipitated. Before cycling, the cell was activated to lessen the influence of interface side reactions. As shown in Fig. 2c and d, the cell exhibited a stable cycling performance. The voltage profiles of the 1st, 10th, 50th and 100th are highly consistent (Fig. 2d). The voltage upper and lower limit stabilized at around 2.2 V and 1.4 V, respectively (Fig. 2c). The molten salt cathode delivered an average discharge specific energy of 155 Wh kg^{-1} (based on the weight of cathode materials) with an average energy efficiency of 83% (Fig. 2e). Both the charge energy density and the discharge energy density remained stable during cycling, which also indicated the high cyclic performance of the whole cell. The XRD results (Fig. 1c) indicate the high

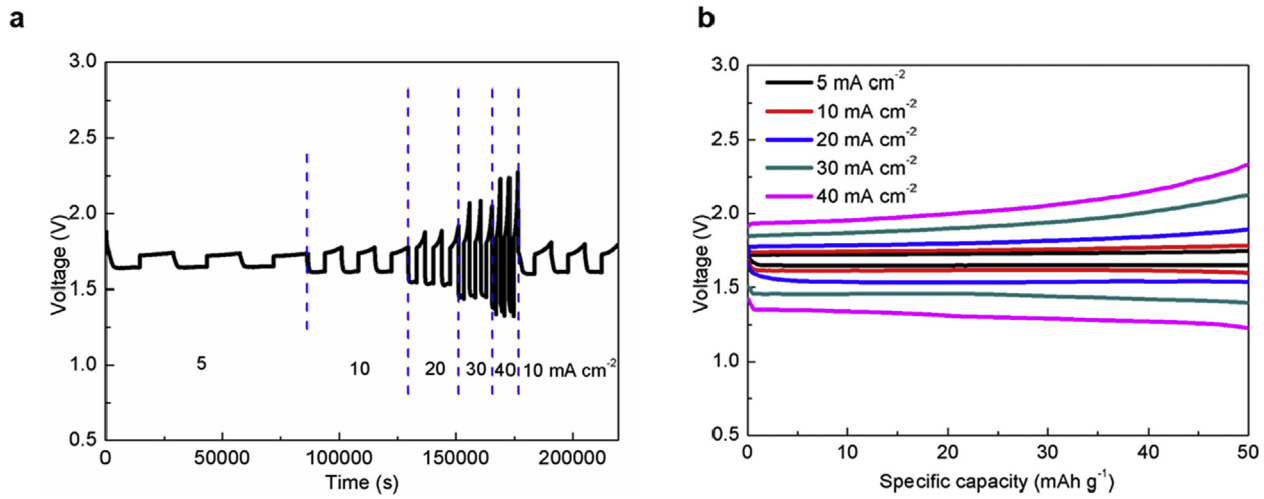

Fig. 3. (a) Voltage profiles of the discharge/charge cycles at various current densities of 5, 10, 20, 30 and 40 mA cm^{-2} with a constant specific capacity of 50 mAh g^{-1}. (b) Voltage as a function of specific capacity at various current densities of 5, 10, 20, 30 and 40 mA cm^{-2} with a constant specific capacity of 50 mAh g^{-1}.

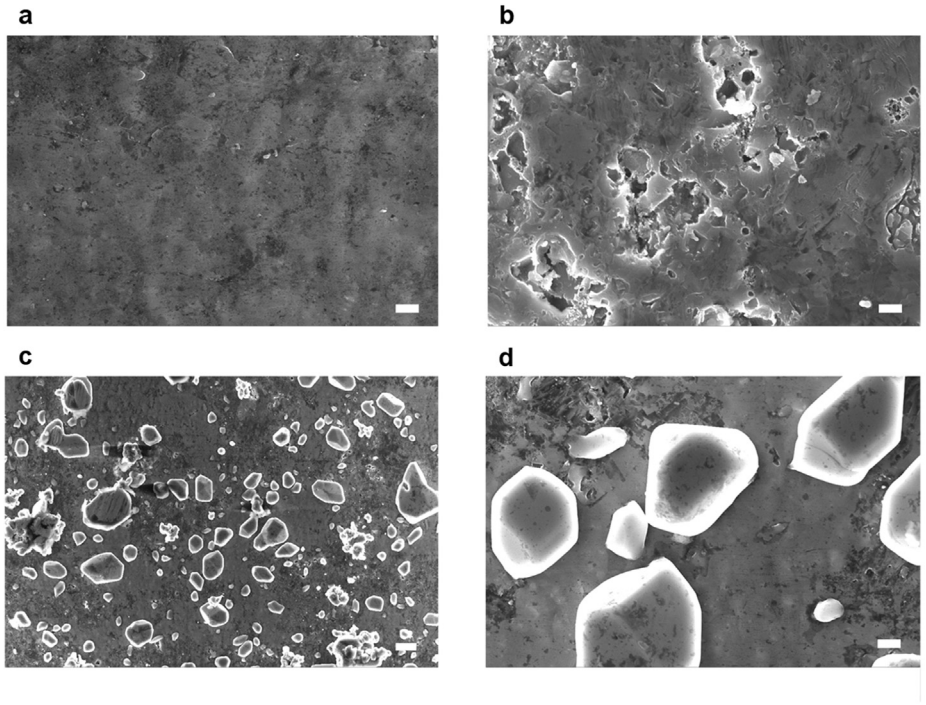

Fig. 4. (a) SEM image of the pristine Al foil. (b) SEM image of the Al foil after the 1st discharge/charge cycle at 10 mA cm^{-2} with a specific capacity of 100 mAh g^{-1}. (c) and (d) SEM images of the Al foil after the 100th cycle at 10 mA cm^{-2} with a specific capacity of 100 mAh g^{-1}. Scale bar, 2 μm (a,b,d) and 10 μm (c).

stability of LLZTO tube during cycling as there is no obvious phase change before and after cycling. To test the safety of the cell in case the LLZTO tube breaks, a puncturing experiment was conducted. The solid electrolyte tube was full of molten $AlCl_3$-LiCl salt (2 g), and the stainless steel case was full of molten lithium (1 g). After heating to 210 °C, the LLZTO tube was punctured, and molten lithium and molten salt was partly contacted. After puncturing, the surface temperature of the stainless steel case increased by only about 50 °C.

The cell was also assembled in the discharge state and part of LiCl was replaced by NaCl to lower the cost. The pristine cathode was composed of LiCl, $AlCl_3$ and NaCl (mole ratio, 4: 1: 1) and little amount of Li was used to connect the LLZTO and the current collector. The cell was firstly charged at 5 mA cm^{-2} with a specific capacity of 200 mAh g^{-1} (Fig. S2a). After the first charge process, the cell delivered a stable cycling performance (Fig. S2b), which indicates that the future cells can be produced without metallic lithium to be handled. Like ZEBRA batteries, all the required active metal can be inserted as salt, therefore the assembling process of the battery can be conducted just in a drying room. The cost of raw materials can be also significantly reduced when the cell is assembled in the discharge state, because metal Li is not indispensable. The impedance test result (Fig. S4) shows that the resistance of the full cell is small and leads to a promising future for the application of this battery.

To smooth the fluctuation of intermittent renewable energy, high rate capability is desired for grid energy storage. The rate performance of the $AlCl_3$-LiCl ||LLZTO|| Li cell was shown in Fig. 3a. The cell was cycled at various current densities from 5 mA cm^{-2} to 40 mA cm^{-2} with a constant discharge/charge capacity of 50 mAh g^{-1}. The voltage profiles at the

current density of 10 mA cm^{-2} showed no obvious changes before and after the cell was cycled at a high current density of 40 mA cm^{-2}, indicating good rate capability of the cell. The discharge plateaus were 1.65, 1.61, 1.54, 1.46 and 1.34 V at current densities of 5, 10, 20, 30 and 40 mA cm^{-2}, respectively (Fig. 3b). Even at a high current density of 40 mA cm^{-2}, the energy efficiency of cell was still higher than 65%. The power density of the $AlCl_3$-LiCl ||LLZTO||Li cell reached 52 mW cm^{-2} at the current density of 40 mA cm^{-2}.

The service life of current collector is also an important factor for rechargeable batteries using in the grid energy storage. In the $AlCl_3$-LiCl|| LLZTO||Li full cell, the Al foil not only functions as positive current collector, but also participates in the reaction. To investigate the stability of the Al current collector, scanning electron microscopy (SEM) was conducted to display the morphology changes of the Al current collector before and after the cycling test. As shown in Fig. 4a, the pristine Al foil was relative smooth with some little protuberances in the surface. After the first discharge/charge cycle, the surface became rough with some corrosion pits (Fig. 4b), which possibly originated from the defects in the surface of the pristine Al foil. After the 100 cycles, there were many particles with the sizes from several micrometers to 30 μm on the surface of the Al current collector (Fig. 4c and d). Energy Dispersive Spectroscopy (EDS) characterization shows that the particles were composed of Al with little amount of oxygen (Fig. S3). The generation of the micron-sized Al particles were partially caused by the inhomogeneous deposition/dissolution of Al during cycles, which possibly led to the loss of the active Al and the corrosion of the current collector. However, the average thickness of the Al foil did not change after the 100 cycles. Even though the thickness of the Al foil used as current collector was only 35 μm, there was no preferable corrosion point. Therefore, the inhomogeneous deposition of Al is not a serious problem for practical applications.

In summary, we demonstrated a newly designed high temperature battery with molten salt cathode-solid electrolyte-molten lithium anode, which can be operated at a relative low temperature of 210 °C with good safety and low cost. The full cell achieved a stable performance for 100 cycles (800 h) with an average energy efficiency of 83% at a current density of 10 mA cm^{-2}. We propose that the cathode material is not limited to $AlCl_3$-LiCl in such battery design; and the battery can be further improved by optimize the molten salt cathode systems in the near future. We anticipate that our $AlCl_3$-LiCl ||LLZTO||Li cells provide new opportunity for large-scale energy storage solutions.

Notes

The authors declare no competing financial interest.

Acknowledgments

The authors would like to appreciate the financial support from the National Basic Research of China (Grants 2015CB932500), National Natural Science Foundations of China (Grant 51661135025 and 51522207). Y. L. would like to thank the support from Tsinghua University Initiative Scientific Research Program.

Appendix A. Supplementary data

Supplementary data to this article can be found online at https://doi.org/10.1016/j.ensm.2019.07.027.

References

[1] P. Fairley, Energy storage: power revolution, Nature 526 (2015) S102–S104.
[2] S. Chu, A. Majumdar, Opportunities and challenges for a sustainable energy future, Nature 488 (2012) 294–303.
[3] S. Chu, Y. Cui, N. Liu, The path towards sustainable energy, Nat. Mater. 16 (2016) 16–22.
[4] B. Dunn, H. Kamath, J.M. Tarascon, Electrical energy storage for the grid: a battery of choices, Science 334 (2011) 928–935.
[5] Z. Yang, J. Zhang, M.C.W. Kintner-Meyer, et al., Electrochemical energy storage for green grid, Chem. Rev. 111 (2011) 3577–3613.
[6] M. Armand, J.M. Tarascon, Building better batteries, Nature 451 (2008) 652–657.
[7] C.D. Parker, Lead–acid battery energy-storage systems for electricity supply networks, J. Power Sources 100 (2001) 18–28.
[8] J.W. Choi, D. Aurbach, Promise and reality of post-lithium-ion batteries with high energy densities, Nat. Rev. Mater. 1 (2016) 16013.
[9] Y. Sun, N. Liu, Y. Cui, Promises and challenges of nanomaterials for lithium-based rechargeable batteries, Nat. Energy 1 (2016) 16071.
[10] X. Dong, L. Chen, J. Liu, et al., Environmentally-friendly aqueous Li (or Na)-ion battery with fast electrode kinetics and super-long life, Sci. Adv. 2 (2016), e1501038.
[11] M.C. Lin, M. Gong, B. Lu, et al., An ultrafast rechargeable aluminium-ion battery, Nature 520 (2015) 324–328.
[12] D.Y. Wang, C.Y. Wei, M.C. Lin, et al., Advanced rechargeable aluminium ion battery with a high-quality natural graphite cathode, Nat. Commun. 8 (2017) 14283.
[13] M. Park, J. Ryu, W. Wang, et al., Material design and engineering of next-generation flow-battery technologies, Nat. Rev. Mater. 2 (2016) 16080.
[14] B. Li, Z. Nie, M. Vijayakumar, et al., Ambipolar zinc-polyiodide electrolyte for a high-energy density aqueous redox flow battery, Nat. Commun. 6 (2015) 6303.
[15] D. Larcher, J.M. Tarascon, Towards greener and more sustainable batteries for electrical energy storage, Nat. Chem. 7 (2015) 19–29.
[16] S. Chu, Y. Cui, N. Liu, The path towards sustainable energy, Nat. Mater. 16 (2017) 16–22.
[17] X. Lu, J.P. Lemmon, J.Y. Kim, et al., High energy density Na–S/NiCl2 hybrid battery, J. Power Sources 224 (2013) 312–316.
[18] K. Wang, K. Jiang, B. Chung, et al., Lithium-antimony-lead liquid metal battery for grid-level energy storage, Nature 514 (2014) 348–350.
[19] H.J. Chang, N.L. Canfield, K. Jung, et al., Advanced Na-NiCl2 battery using nickel-coated graphite with core–shell microarchitecture, ACS Appl. Mater. Inter. 9 (2017) 11609–11614.
[20] C.H. Dustmann, Advances in ZEBRA batteries, J. Power Sources 127 (2014) 85–92.
[21] Y. Jin, K. Liu, J. Lang, et al., An intermediate temperature garnet-type solid electrolyte-based molten lithium battery for grid energy storage, Nat. Energy 3 (2018) 732.
[22] G. Li, X. Lu, J.Y. Kim, et al., An advanced Na–FeCl2 ZEBRA battery for stationary energy storage application, Adv. Energy Mater. 5 (2015) 1500357.
[23] M.S. Park, S.B. Ma, D.J. Lee, et al., A highly reversible lithium metal anode, Sci. Rep. 4 (2014) 3815.
[24] X. Han, Y. Gong, K.K. Fu, et al., Negating interfacial impedance in garnet-based solid-state Li metal batteries, Nat. Mater. 16 (2017) 572–579.
[25] V. Thangadurai, D. Pinzaru, S. Narayanan, A.K. Baral, Fast solid-state Li ion conducting garnet-type structure metal oxides for energy storage, J. Phys. Chem. Lett. 6 (2015) 292–299.
[26] V. Thangadurai, H. Kaack, W.J.F. Weppner, Novel fast lithium ion conduction in garnet-type Li5La3M2O12 (M=Nb, Ta), J. Am. Ceram. Soc. 86 (2003) 437–440.
[27] J. Kim, D. Shin, Y. Jung, S.M. Hwang, T. Song, Y. Kim, Paik, U. LiCl-LiI molten salt electrolyte with bismuth-lead positive electrode for liquid metal battery, J. Power Sources 377 (2018) 87–92.